Materials Today Communications 38 (2024) 108004

Contents lists available at ScienceDirect

Materials Today Communications

journal homepage: www.elsevier.com/locate/mtcomm

# Dependence of magnetic performance on coating method in grain boundary diffusion processed Nd-Fe-B sintered magnets

Jaehyuk kim [a,b,1], Ye Ryeong Jang [c,1], Dong Hyun Lee [a,d], Seong Chan Kim [a,b], Ju-Young Beak [a], Donghwan Kim [e], Sang Hyub Lee [e], Sumin Kim [f], Jong Wook Roh [d], Wooyoung Lee [c], Dalhyun Do [b], Dong Hwan Kim [a,*], Jeongmin Kim [a,*]

[a] Division of Nanotechnology, DGIST, 333 Techno Jungang-daero, Hyeonpung-eup, Dalseong-gun, Daegu 42988, Republic of Korea
[b] Department of Advanced Materials Engineering, Keimyung University, 1095, Dalgubeol-daero, Dalseo-gu, Republic of Korea
[c] Department of Materials Science and Engineering, Yonsei University, 50 Yonsei-ro, Seodaemoon-gu, Seoul 03722, Republic of Korea
[d] School of Nano and Materials Science and Engineering, Kyungpook National University, Gyeongsangbuk-do 37224, Republic of Korea
[e] R&D Center, Star Group, Daegu 42714, Republic of Korea
[f] Department of Magnetic Materials, Korea Institute of Materials Science, Changwon 51508, Republic of Korea

ARTICLE INFO

*Keywords:*
Grain boundary diffusion
Nd–Fe–B
Coating method
Coercivity
Remanence

ABSTRACT

In this study, commercial sintered Nd–Fe–B magnets were coated with a grain-boundary-diffusion HRE source ($TbH_x$) using two different approaches, and the resulting variations in the magnetic properties were systematically investigated. The coercivity increased significantly from 12.8 to 24.4 kOe and to 26.8 kOe by enabling $TbH_x$ diffusion through dip and spray coating, respectively. Slight diffusion-induced decreases in remanence were observed for the dip- and spray-coated magnets, from 14.5 to 14.0 kG and to 14.3 kG, respectively. Microstructural analysis indicated that the spray-coated magnet exhibited performance superior to that of its dip-coated counterpart; this was likely due to the mitigation of the low-efficiency diffusion from the side-wall coating, in which the direction of diffusion—which was perpendicular to the alignment orientation of the magnet—promoted diffusion through the grain interior rather than along the grain boundaries.

## 1. Introduction

The growth of environmentally friendly mobility systems, including electric vehicles, robots, and drones, has accelerated the demand for high-performance Nd–Fe–B permanent magnets. These magnets must exhibit high coercivity to operate reliably at the working temperatures of driving motors, that is, 150–200 °C [1]. However, the coercivity of these systems typically decreases at such high temperatures; nevertheless, to overcome this issue, heavy rare earth (HRE) elements such as Tb and Dy have been added to the $Nd_2Fe_{14}B$ main phase to exploit the high anisotropy field of the $HRE_2Fe_{14}B$ phase [2]. However, the addition of Tb or Dy leads to a decrease in remanence owing to the antiferromagnetic coupling between the HREs and Fe [3,4].

Grain boundary diffusion (GBD) treatment was developed to enhance the coercivity of sintered Nd–Fe–B magnets without causing a considerable decrease in remanence [5,6]. In this heat-treatment method, the HRE diffusion source is coated onto the surfaces of the magnet, enabling HRE diffusion along the grain boundaries and formation of $(Nd, HRE)_2Fe_{14}B$ shell structures on the surface of grains by replacing Nd in the main phase. The formation of core–shell structures not only preserves the remanence, but also dramatically reduces the HRE consumption for enhancing coercivity via HRE addition [7–10].

The GBD treatment performed to comprehensively infiltrate diffusion materials into the matrix through grain boundaries begins with uniformly positioning the HRE diffusion source on the magnet surface [11]. The simplest method involves attaching a metal sheet directly to the magnet surface, which provides straightforward control over the direction of diffusion as well as enables the use of diffusion materials that are difficult to employ powder processing [12–14]. However, this method consumes a substantial amount of the diffusing HRE source owing to the post-diffusion production of residues; moreover, it is not suitable for the continuous mass production of magnets.

The residues on the magnet surface appearing after diffusion can be minimized using vapor deposition processes enabling precise control of

* Corresponding authors.
*E-mail addresses:* kimdhwan@dgist.ac.kr (D.H. Kim), jkim@dgist.ac.kr (J. Kim).
[1] J. Kim and Y. R. Jang contributed equally to this work.

https://doi.org/10.1016/j.mtcomm.2023.108004
Received 12 November 2023; Received in revised form 18 December 2023; Accepted 29 December 2023
Available online 2 January 2024

the HRE source coating, such as evaporation [15], sputtering [16,17], and ion plating [11]. These vacuum-based methods guarantee a high-purity diffusion source for GBD, and they are sustainable liquid-waste-free processes; however, they are expensive and not amenable to mass production [18,19].

To make GBD compliant with the mass production of sintered magnets, continuous coating techniques—such as dipping and spraying with slurry-type HRE sources—are the most effective [20,21]. In these methods, the diffusion materials synthesized by powder processing are mixed with alcohol, coated onto the magnet surface, and then dried. This wet process is suitable for large-scale magnets, and the magnitude of the HRE source coating can be easily controlled by adjusting the slurry concentration [22]. Recently, a simpler and more convenient technique has been reported for applying dried powder; however, it has limitations in terms of ensuring uniform application and adequate adhesion between the diffusion material and the magnet surface [23,24].

In this study, the ways in which the magnetic performance of GBD-processed sintered Nd–Fe–B magnets depended on the coating method were systematically investigated using $TbH_x$-based dip and spray coating. For identical amounts of the HRE source, the spray-coated magnet subjected to HRE GBD showed a greater increase in coercivity than that of its dip-coated counterpart. Moreover, the remanence reduction caused by the HRE GBD was slightly less in spray coating than in dip coating. Microstructural and elemental distribution analyses indicated that these coating-method-related differences were due to anisotropic diffusion in the crystallographically aligned magnet. Overall, this study offers a mass-production-enabling coating method that can reduce the HRE source consumption and HRE utilization.

## 2. Experimental

Commercial N52-grade Tb-free sintered magnets with dimensions of $12 \times 12 \times 5$ $mm^3$ were used as the original magnets. The HRE diffusion source was prepared by induction melting Tb granules in vacuum and then hydrogenating the product at 600 °C for 6 h. The obtained $TbH_x$ compounds were pulverized by ball milling and then mixed with ethanol in a mass ratio of 1:4 to prepare a slurry. Basket milling was conducted thereafter at 850 rpm for 3 h to yield fine 1–10-μm-sized particles. The original magnets were coated with the $TbH_x$ slurry (0.2–0.7 wt%) on all surfaces and on the top and bottom surfaces normal to the aligned direction of magnet through dip and spray coating, respectively (Fig. 1). $TbH_x$ less than 0.8 wt% was used in both coating methods to exclude the effects of agglomeration of the diffusion source. GBD treatment was performed in vacuum ($10^{-6}$ Torr) at 800 °C for 6 h and then at 900 °C for 14 h using a custom-made vacuum furnace, and the GBD-processed magnets were annealed at 450 °C for 3 h. The magnetic properties of the resulting systems were measured using a BH tracer (Permagraph C-300, Magnet-Physik), whereas microstructure and elemental distribution analyses were conducted by scanning electron microscopy (SEM; SU8220, Hitachi), field-emission electron probe microanalysis (FE-EPMA; JAX8530F, JEOL), and energy-dispersive spectrometry (EDS; JSM7800F).

## 3. Result and discussion

Demagnetization curves were acquired for the original magnet, magnet heat-treated in the absence of $TbH_x$, and $TbH_x$ (0.7 wt %)-diffused magnets subjected to dip and spray coating (Fig. 2(a)). The room-temperature coercivity $H_{cj}$ increased from 12.79 kOe (for the pristine specimen) to 24.35 and 26.84 kOe (for the dip- and spray-coated magnets, respectively; Fig. 2(b)). Notably, a value of 15.25 kOe was obtained for the magnet that underwent the same heat-treatment protocol without $TbH_x$, which indicated that the significant increase in the coercivity of the Tb-diffused magnets was due to the Tb-diffusion-induced formation of a (Nd, Tb)$_2$Fe$_{14}$B phase with a high anisotropy field [25]. In particular, the spray-coated magnet showed a noticeably higher enhancement in coercivity than that of its dip-coated counterpart ($\Delta H_{cj}$ = 14.05 and 11.56 kOe, respectively), indicating that the GBD-induced improvement in the magnetic properties varied with the coating method. The remanence of the magnets ($B_r$) decreased slightly from the original value of 14.51 kG to 14.48, 14.03, and 14.25 kG for the Tb-free, dip-coated, and spray-coated samples, respectively. Notably, spray coating achieved a smaller Tb-diffusion-induced reduction in remanence than that of dip coating.

The magnetic properties of the original, Tb-free, and Tb-diffused magnets prepared by dip and spray coating were assessed based on their thermal stability at 25–200 °C (Fig. 2(c) and (d)). The remanence and coercivity decreased gradually with increasing temperature, as observed in typical Nd–Fe–B magnets; however, the temperature coefficients of remanence and coercivity ($\alpha$ and $\beta$, respectively) were improved by the heat treatment and Tb diffusion [26,27]. In particular, the $\beta$ values of the diffused magnets showed remarkable improvements, presumably owing to the enhanced anisotropy field generated by the formation of the (Nd, Tb)$_2$Fe$_{14}$B phase at the surface of grains [28]. Furthermore, the thermal stability of the original specimen ($\alpha$ and $\beta$: –0.216 and –0.531 %/°C, respectively) improved to a greater extent upon spray coating ($\alpha$ and $\beta$: –0.209 and –0.477 %/°C, respectively) than upon dip coating ($\alpha$ and $\beta$: –0.211 and –0.482 %/°C, respectively).

For the original, Tb-free, and $TbH_x$ (0.7 wt%)-diffused magnets obtained by dip and spray coating, SEM images were acquired in back-scattered electron (BSE) mode and the corresponding EPMA-derived Fe, Nd, O, and Tb distributions were determined at a depth of 100 μm from the magnet surface (Fig. 3). In the original magnet, boundaries between the <10-μm-diameter grains were not clearly observed, and the matrix comprised Nd$_2$Fe$_{14}$B main phases (dark regions) and Nd-rich phases at triple junctions (bright regions), according to the elemental mapping (Fig. 3(a)). It is worth noting that the residual oxygen introduced during sintered magnet processes is present predominantly in the Nd-rich phase [29,30], with the heat treatment enabling the distribution of the low-melting-point Nd-rich phase on the grain boundaries [31]. The separation of grains, including those with extremely thin boundaries having an Nd-rich phase, was observed in the magnet heat-treated in the absence of $TbH_x$ (Fig. 3(b)). The continuous distribution of the nonmagnetic Nd-rich phase diminished the magnetization coupling effect between the grains by isolating the Nd–Fe–B phase, leading to an increase in coercivity, as shown in Fig. 2 [32]. In this heat-treatment

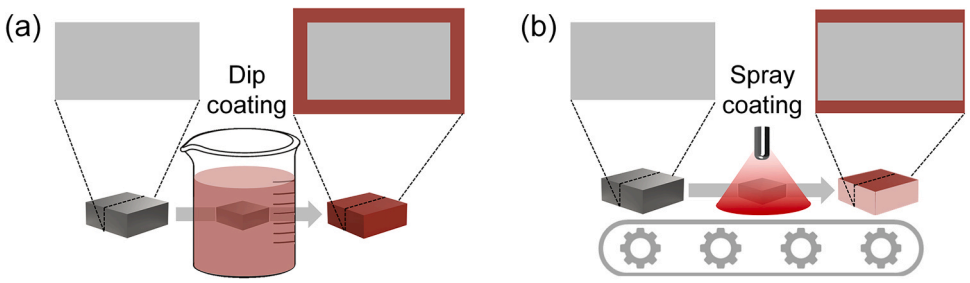


**Fig. 1.** Schematic illustrations of (a) dip and (b) spray coating processes and the coating features.

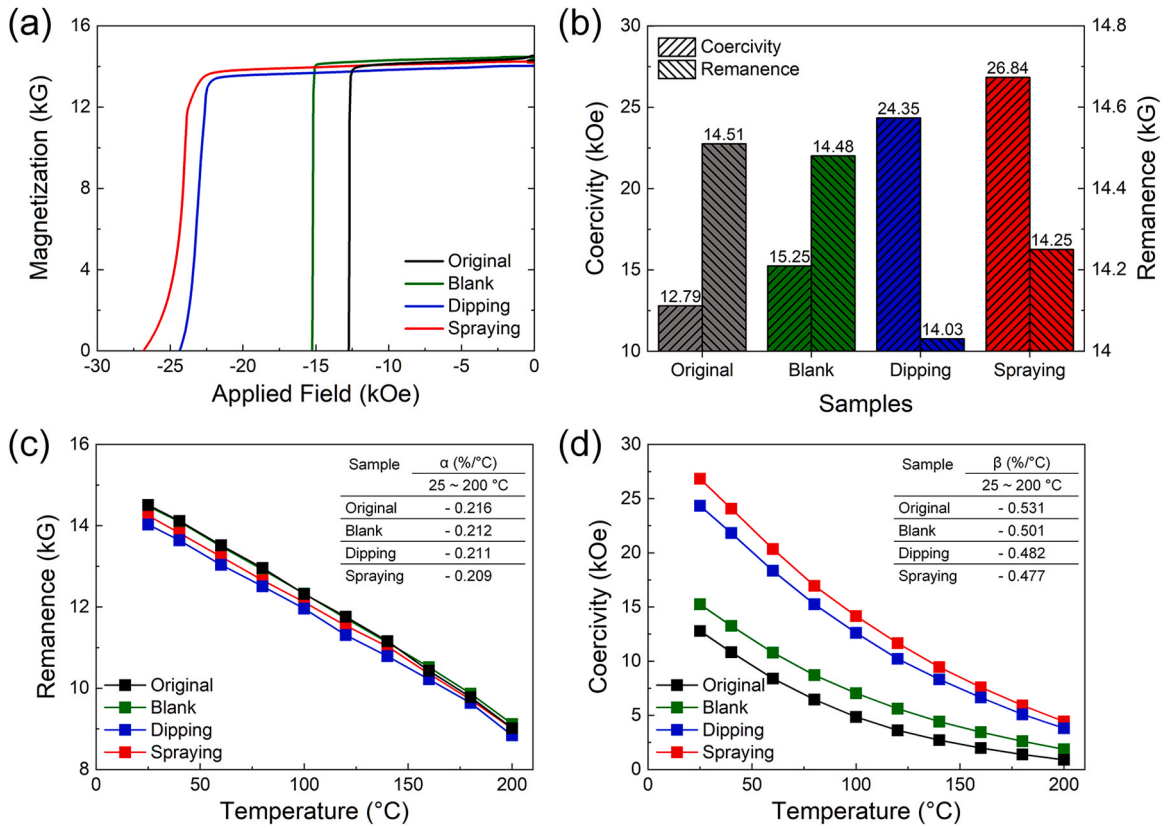


**Fig. 2.** (a) Demagnetization curves of the original magnets, magnets heat-treated without $TbH_x$, and magnets dip- and spray-coated with 0.7 wt% $TbH_x$ at room temperature. (b) Variations in the coercivity and remanence of the magnets induced by the heat treatment and GBD. Temperature-dependent (c) remanence and (d) coercivity of the magnets.

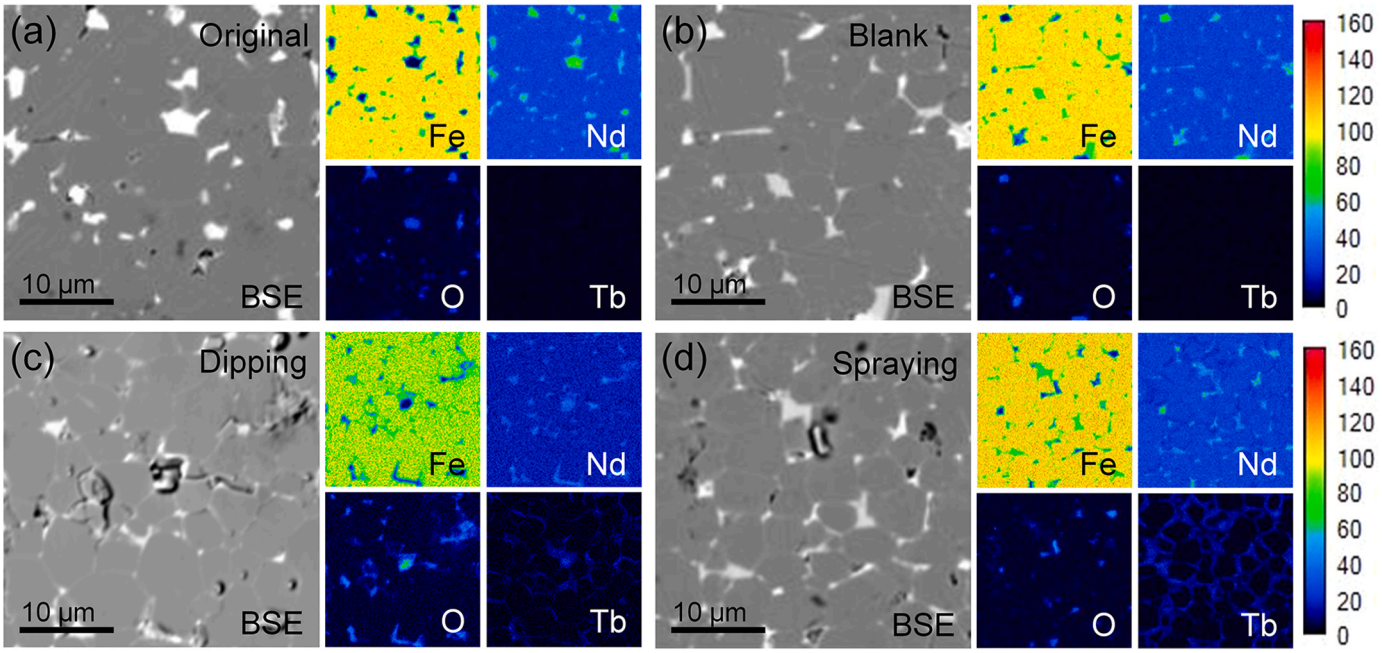


**Fig. 3.** BSE-SEM and EPMA images showing the distributions of Fe, Nd, O, and Tb in the (a) original, (b) $TbH_x$-free heat-treated, (c) dip-coated, and (d) spray-coated magnets at a depth of 100 μm from the magnet surface.

method, the grain size of the original magnet was maintained without leading to unintended grain coarsening.

SEM images of the $TbH_x$-diffused magnets showed even more distinct and continuous grain boundaries compared with those in the original and Tb-free heat-treated magnets (Fig. 3(c) and (d)). The corresponding elemental distributions revealed a thick (Nd, $Tb)_2Fe_{14}B$ shell (gray regions), which was formed by the GBD of Tb, around the Nd–Fe–B core. The unambiguous core–shell structures effectively inhibited the

nucleation of the reversed domain on the grain surface, dramatically enhancing the coercivity of the diffused magnets, along with the magnetic decoupling effect of the continuous Nd-rich grain boundaries, as shown in Fig. 2 [33–35].

Notably, the spray-coated Tb-diffused magnet had a thicker shell than that of its dip-coated counterpart, despite the identical amounts of the HRE source coating (~0.7 wt%). This was presumably due to the asymmetric coating produced during spraying. In contrast to dip coating, in which a uniform amount per unit area was coated on all sides of the magnet (Fig. 1(a)), spray coating predominantly applied the diffusion source to the upper and lower surfaces perpendicular to the *c*-axis, thereby facilitating GBD (Fig. 1(b)). This advantage, which further enhanced the coercivity through spraying, was confirmed by the dependence of the magnetic properties on the amount of coating.

The magnetic properties of the Tb-diffused magnets obtained by dip and spray coating were investigated with respect to the amount of the diffusion source (Fig. 4). For both Tb-diffused magnets, the coercivity gradually increased from the value of the Tb-free magnet with increasing $TbH_x$ amount from 0 to 0.7 wt% (Fig. 4(a)). In particular, the coercivity of the spray-coated magnet was higher than that of its dip-coated equivalent throughout the investigated coating amount range. Considering the enhancement in coercivity due to the formation of the $(Nd, Tb)_2Fe_{14}B$ phase with a high anisotropy field, this result indicated that spray coating led to greater Tb infiltration of the magnet matrix than that achieved by dip coating. This is consistent agreement with the Tb mapping results (Fig. 3(c) and (d)).

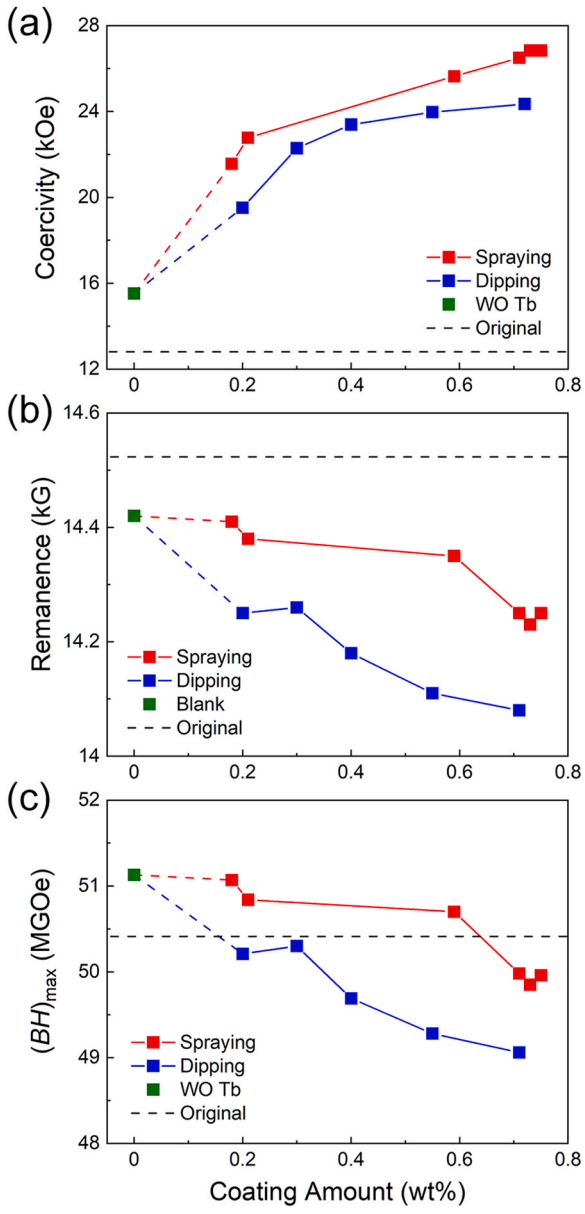


**Fig. 4.** Variations in the (a) coercivity, (b) remanence, and (c) maximum energy product ($(BH)_{max}$) values of the Tb-diffused magnets obtained by dip and spray coating with respect to the amount of the diffusing source being coated.

Notably, the Tb-diffusion-induced formation of the $(Nd, Tb)_2Fe_{14}B$ phase is accompanied by a decrease in remanence owing to the antiferromagnetic coupling between the Tb and Fe [3,4]. Therefore, the remanence values of the Tb-diffused magnets obtained using both coating methods decreased with increasing coating amount (Fig. 4(b)). However, the remanence values of the spray-coated magnets with greater Tb infiltration were noticeably higher than those of the dip-coated magnets over the entire coating amount range. This suggests that the superior enhancement of magnetic properties for the spray-coated magnet originated not only in the asymmetric coating produced by the spraying, but also in the different diffusion mechanisms that depended on the magnet surface. The dependences of the diffusion mechanism and efficiency on the diffusion-initiating plane are discussed comprehensively in the subsequent section (see the Fig. 5 discussion).

The maximum energy product ($(BH)_{max}$) of the Tb-diffused magnets was subsequently examined (Fig. 4(c)). Although, the $(BH)_{max}$ values decreased gradually from 51.13 MGOe (for the Tb-free system) to 49.06 and 49.96 MGOe (for the dip- and spray-coated magnets, respectively) with increasing coating amount, the reduction in $(BH)_{max}$ for the magnet spray-coated with 0.7 wt% $TbH_x$—which exhibited the highest coercivity among the specimens—was less than that of the original magnet (50.41 MGOe) by only 0.5 MGOe. Furthermore, similar to the coercivity and remanence results, the $(BH)_{max}$ values of the spray-coated magnets were higher than those of the dip-coated magnets across the entire coating amount range.

The distributions and concentrations of Tb were analyzed at depths of 50, 100, and 150 μm with respect to the diffusion-initiating surface of the dip- and spray-coated magnets (Fig. 5). According to the results (Fig. 5(a) and (b)), the thickness of the $(Nd, Tb)_2Fe_{14}B$ shell decreased with increasing distance from the magnet surface. In the case of diffusion from the upper and lower surfaces normal to the *c*-axis of the magnet matrix, the spray-coated magnet had thicker shell structures than those of the dip-coated magnet, which was also evident in the Tb concentration vs. depth profiles (Fig. 5(c)). This was presumably due to the greater application of the $TbH_x$ onto the upper and lower surfaces through the asymmetric spraying, despite the use of an identical amount of the diffusion source in the dip coating. Similarly, the shell formed by diffusion initiated from the side surface was thinner for spray coating than for dip coating due to the less $TbH_x$ application, which was clearly confirmed by the depth-dependent Tb concentration (Fig. 5(d)).

The HRE GBD—in which HRE atoms infiltrate the magnet matrix, diffuse through the Nd-rich grain boundary phase, and replace Nd atoms of the $Nd_2Fe_{14}B$ main phase—can occur through two distinct mechanisms: diffusion through grain boundary and lattice. The lattice diffusion that enables the $(Nd, HRE)_2Fe_{14}B$ shell formation is strongly dependent on the orientation of the anisotropic $Nd_2Fe_{14}B$ crystal structure. The distance between adjacent Nd atoms in the plane normal to the *c*-axis was considerably less than that along the *c*-axis, which determines the diffusion length required for Tb to substitute for Nd. Moreover, the energy barrier enabling diffusion normal to the *c*-axis was found to be smaller than that in the parallel direction. T. Kim *et al.* calculated the direction-dependent energy barrier of Dy diffusion relatively simply by using a harmonic spring model with a spring constant ($k$) [36]. For Tb diffusion, the energy barrier perpendicular to the *c*-axis ($1/2k0.0023$) was found to be about 5 times less than that in the parallel direction ($k0.0058$). Therefore, the Tb infiltration from the side surfaces of the *c*-axis-aligned magnet promotes lattice diffusion, which consumes Tb and thereby reduces the GBD efficiency. Consequently, in the

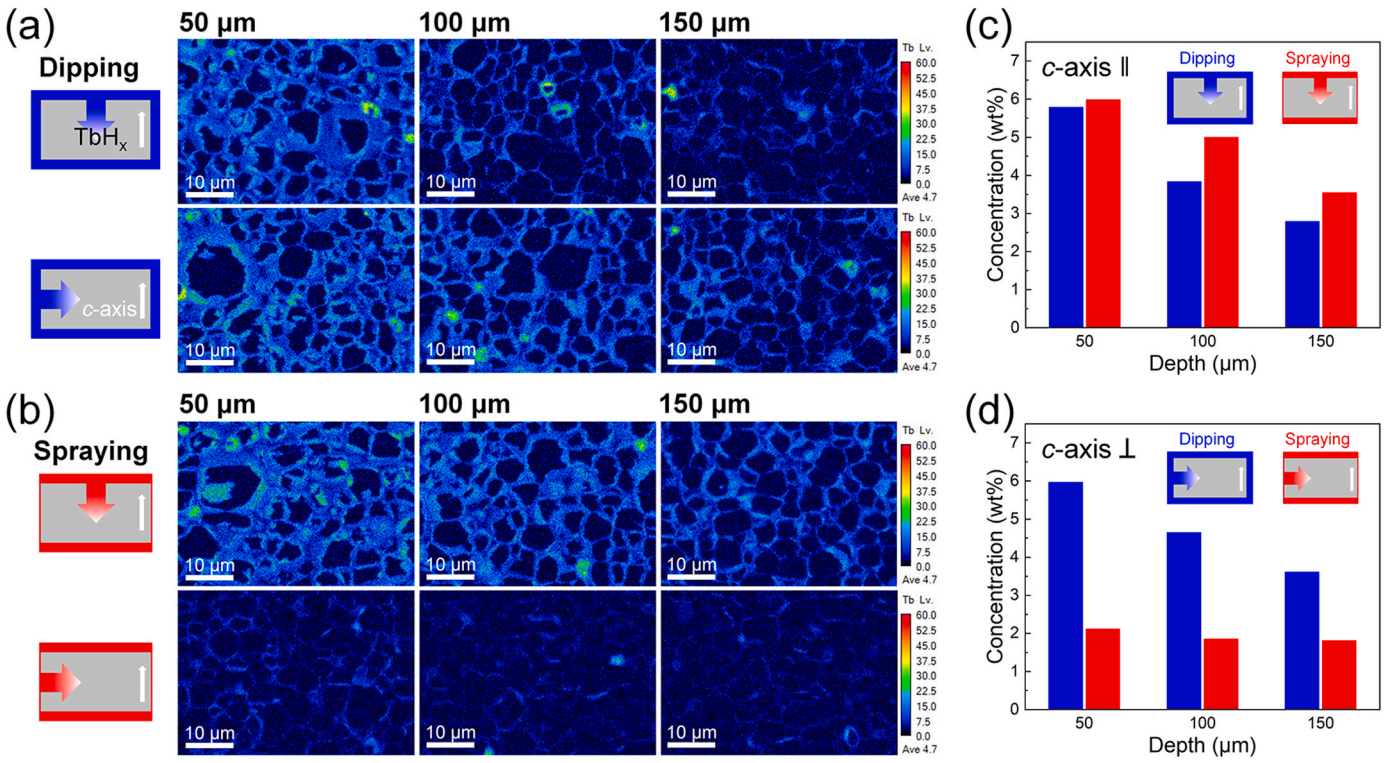


**Fig. 5.** EPMA images showing the Tb distribution in the (a) dip- and (b) spray-coated magnets at depths of 50, 100, and 150 μm for two different diffusion-initiating approaches. The Tb concentration of the dip- and spray-coated magnets as a function of the depth from the surfaces (c) perpendicular and (d) parallel to the magnetic alignment direction of the magnet (*c*-axis).

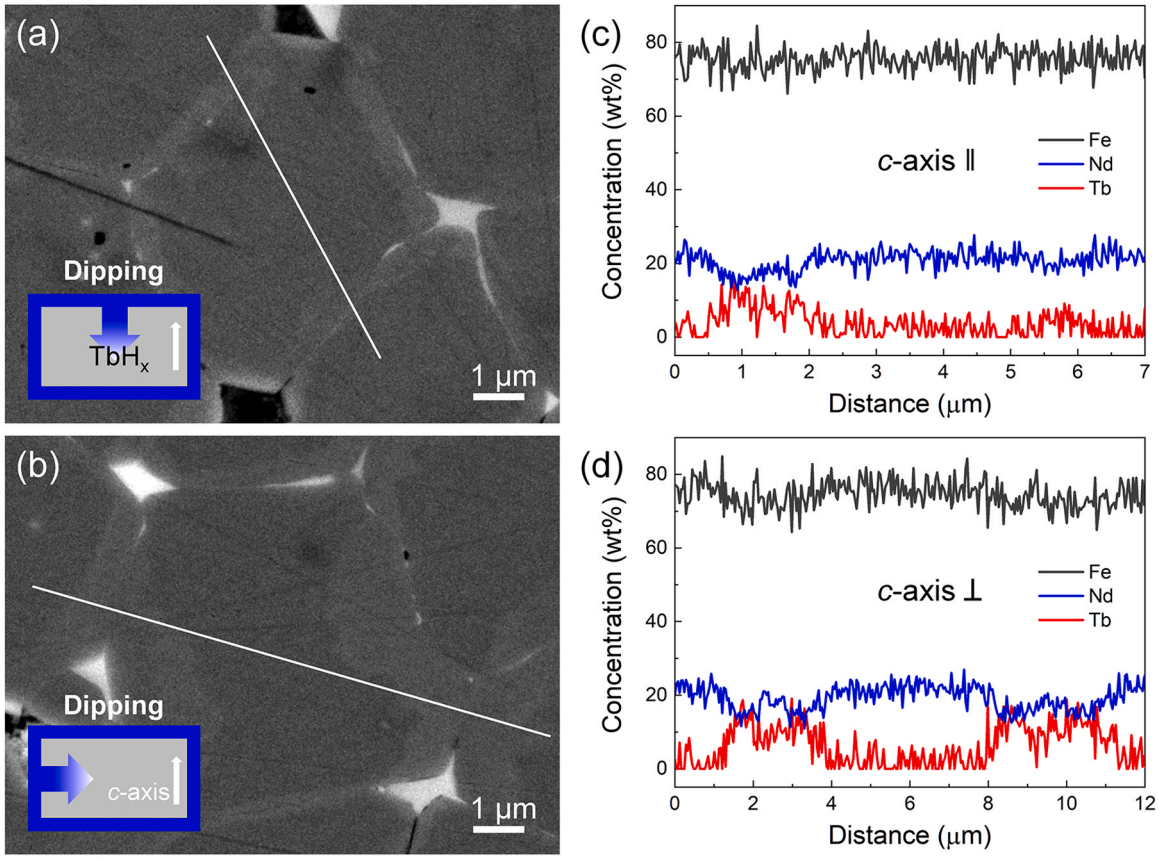


**Fig. 6.** BSE-SEM images of the Tb-diffused magnet prepared by dip coating acquired at a depth of 50 μm from the (a) top and (b) side diffusion-initiating surfaces, and (c, d) the corresponding line distributions of Fe, Nd, and Tb obtained by EDS scanning along the white line shown in the SEM images.

dip-coated magnet with symmetrically covered entire surfaces, the (Nd, Tb)$_2$Fe$_{14}$B shell formed by diffusion from the side surface was thicker than that formed by the top-surface coating (Fig. 5(a)); this was quantitatively confirmed by comparing the analyzed Tb concentrations (Fig. 5(c) and (d)).

Finally, to confirm the excessive lattice diffusion originating from the side-surface coating, the (Nd, Tb)$_2$Fe$_{14}$B shell structures were investigated according to the diffusion-initiating surfaces for the dip-coated magnet with symmetric coverage. BSE-SEM images of a representative core–shell-structured grain in the dip-coated magnet were acquired at a depth of 50 μm from the top and side surfaces (Fig. 6(a) and (b), respectively). In the case of diffusion from the top surface, a relatively thin and uniform shell was observed, whereas side-surface diffusion showed dominant shell growth on the plane parallel to the *c*-axis owing to anisotropic lattice diffusion. The corresponding line distributions of Fe, Nd, and Tb were determined for the top- and side-surface diffusion (Fig. 6(c) and (d), respectively). The line-scan directions were slightly tilted with respect to the diffusion trajectory to investigate the shell/grain-boundary/shell structures. The increase and decrease in Tb and Nd concentrations, respectively, indicated that Tb atoms diffused along the grain boundaries and substituted Nd atoms in the main phase. Moreover, a Tb-rich/Nd-rich/Tb-rich structure was clearly observed in the case of side-surface diffusion (Fig. 6(d)). Furthermore, the line-scan results suggested that the shell formed near the side surface was not only thicker (~3 μm) than that near the top surface (<2 μm), but also exhibited a higher Tb concentration (Figs. 6(c) and 5(d)).

This excessive lattice diffusion of Tb caused by side-surface coating aggravated the remanence deterioration owing to the antiferromagnetic coupling [37–39]. Therefore, the Tb-diffused magnets with asymmetric spray-coated surfaces, which were predominantly coated on the top and bottom surfaces normal to the *c*-axis, exhibited higher remanence as well as coercivity values than those of the dip-coated magnets for the same amount of the diffusion source (Fig. 4(a) and (b)). Additionally, more than 1 wt% TbH$_x$ was required in dip coating to achieve the coercivity of the magnet spray-coated with 0.7 wt% TbH$_x$, which also led to a further decrease in remanence. The coercivity of the magnet was found to be 26.60 kOe for the 1.05 wt% TbH$_x$ in this overcoating test based on dipping, which indicated a ~30% reduction in HRE utilization compared to that of the spray-coated magnet (26.84 kOe) with 0.73 wt % TbH$_x$.

## 4. Conclusion

In this study, the manner in which the magnetic properties of sintered Nd–Fe–B magnets were influenced by the HRE-source-coating method conducted to enable HRE GBD was systematically investigated, and the advantages of the widely used spray-coating process for mass production of these magnets were clearly revealed. While dip coating led to the HRE source being uniformly coated on all surfaces of the original magnet, asymmetric spraying resulted in a predominant coating on the target surface with high GBD efficiency. This technical advantage led to an additional increase in coercivity for the same diffusion source. Moreover, the asymmetric coating minimized HRE diffusion in the direction perpendicular to the *c*-axis of the magnet matrix, restricting the deterioration of remanence caused by excessive lattice diffusion. Consequently, the magnets spray-coated with TbH$_x$ exhibited coercivity, remanence, and maximum energy product values superior to those of magnets dip-coated with the same amount of TbH$_x$, leading to a 30 % reduction in HRE utilization for achieving the same coercivity enhancement. Consequently, the asymmetric spray-coating amplified the HRE-GBD-induced coercivity enhancement and effectively inhibited the accompanying remanence reduction.

## CRediT authorship contribution statement

**Kim Jeongmin:** Conceptualization, Funding acquisition, Investigation, Methodology, Supervision, Writing – original draft, Writing – review & editing. **Jang Ye Ryeong:** Methodology, Writing – original draft. **Lee Dong Hyun:** Investigation, Methodology, Validation. **Do Dalhyun:** Investigation, Validation. **Kim Dong Hwan:** Funding acquisition, Investigation, Methodology, Writing – review & editing. **Kim Jaehyuk:** Investigation, Methodology, Writing – original draft. **Kim Seong Chan:** Investigation, Methodology, Validation. **Beak Ju-Young:** Formal analysis, Methodology. **Kim Donghwan:** Investigation, Methodology, Resources. **Roh Jong Wook:** Investigation, Validation. **Lee Wooyoung:** Investigation, Validation. **Lee Sang Hyub:** Investigation, Methodology, Resources. **Kim Sumin:** Formal analysis, Methodology, Validation.

## Declaration of Competing Interest

The authors declared that they have no conflicts of interest to this work. We declare that we do not have any commercial or associative interest that represents a conflict of interest in connection with the work submitted.

## Data Availability

No data was used for the research described in the article.

## Acknowledgments

This work was supported by the DGIST R&D Program (23-DPIC-01) and the National Research Foundation of Korea (NRF) (RS-202300238493).

## References

[1] Y. Matsuura, Recent development of Nd–Fe–B sintered magnets and their applications, J. Magn. Magn. Mater. 303 (2) (2006) 344–347.
[2] M. Sagawa, S. Hirosawa, H. Yamamoto, S. Fujimura, Y. Matsuura, Nd鋀fe鋀b permanent magnet materials, Jpn. J. Appl. Phys. 26 (6R) (1987) 785–800.
[3] B. Chen, X. Liu, R. Chen, S. Guo, C. Yan, D. Lee, A. Yan, Design and fabrication of Dy-free sintered permanent magnets with high coercivity, J. Appl. Phys. 111 (7) (2012) 07A710.
[4] C.H. Lin, S.K. Chen, K.D. Lin, W.C. Chang, T.S. Chin, Magnetic properties and microstructure of magnesium-doped Nd-Fe-B magnets, J. Appl. Phys. 64 (10) (1988) 5513–5515.
[5] X. Pan, A manufacturing method of magnet with the world's highest heat-resistance developed by Japan, Funct. Mater. Inf. 2 (3) (2005) 61.
[6] K. Hirota, H. Nakamura, T. Minowa, M. Honshima, Coercivity enhancement by the grain boundary diffusion process to Nd-Fe-B sintered magnets, IEEE Trans. Magn. 42 (10) (2006) 2909–2911.
[7] H. Sepehri-Amin, T. Ohkubo, K. Hono, Grain boundary structure and chemistry of Dy-diffusion processed Nd–Fe–B sintered magnets, J. Appl. Phys. 107 (9) (2010) 09A745.
[8] H. Sepehri-Amin, T. Ohkubo, K. Hono, The mechanism of coercivity enhancement by the grain boundary diffusion process of Nd–Fe–B sintered magnets, Acta Mater. 61 (6) (2013) 1982–1990.
[9] H. Suzuki, Y. Satsu, M. Komuro, Magnetic properties of a Nd–Fe–B sintered magnet with Dy segregation, J. Appl. Phys. 105 (7) (2009) 07A734.
[10] W.F. Li, H. Sepehri-Amin, T. Ohkubo, N. Hase, K. Hono, Distribution of Dy in high-coercivity (Nd,Dy)–Fe–B sintered magnet, Acta Mater. 59 (8) (2011) 3061–3069.
[11] J. He, J. Cao, Z. Yu, W. Song, H. Yu, M. Hussain, Z. Liu, Grain boundary diffusion sources and their coating methods for Nd-Fe-B permanent magnets, Metals (2021).
[12] K. Lu, X. Bao, M. Tang, G. Chen, X. Mu, J. Li, X. Gao, Boundary optimization and coercivity enhancement of high (BH)max Nd-Fe-B magnet by diffusing Pr-Tb-Cu-Al alloys, Scr. Mater. 138 (2017) 83–87.
[13] K. Loewe, D. Benke, C. Kübel, T. Lienig, K.P. Skokov, O. Gutfleisch, Grain boundary diffusion of different rare earth elements in Nd-Fe-B sintered magnets by experiment and FEM simulation, Acta Mater. 124 (2017) 421–429.
[14] L. Jin, G. Ding, J. Zhu, Z. Jin, B. Zheng, S. Guo, R. Chen, A. Yan, X. Liu, Effective microstructure optimization and coercivity enhancement of sintered Nd–Fe–B magnet by grain boundary diffusion of Pr60Tb13Al27 alloy, J. Alloys Compd. 870 (2021) 159375.
[15] N. Watanabe, H. Umemoto, M. Ishimaru, M. Itakura, M. Nishida, K. Machida, Microstructure analysis of Nd-Fe-B sintered magnets improved by Tb-metal vapour sorption, J. Microsc. 236 (2) (2009) 104–108.
[16] D. Li, S. Suzuki, T. Kawasaki, K.I. Machida, Grain interface modification and magnetic properties of Nd-Fe-B sintered magnets, Jpn. J. Appl. Phys. 47 (10 PART 1) (2008) 7876–7878.

[17] K. Matchida, S. Suzuki, T. Kawasaki, D.S. Li, T. Kitamon, K. Nakamura, Y. Shimizu, High-coercive Nd-Fe-B sintered magnets diffused with Dy or Tb metal and their applications, 2005 IEEE Int. Magn. Conf. (INTERMAG) (2005) 947–948.
[18] S. Lee, J. Kwon, H.-R. Cha, K.M. Kim, H.-W. Kwon, J. Lee, D. Lee, Enhancement of coercivity in sintered Nd-Fe-B magnets by grain-boundary diffusion of electrodeposited Cu-Nd Alloys, Met. Mater. Int. 22 (2) (2016) 340–344.
[19] B. Navinšek, P. Panjan, I. Milošev, PVD coatings as an environmentally clean alternative to electroplating and electroless processes, Surf. Coat. Technol. 116-119 (1999) 476–487.
[20] F. Chen, Recent progress of grain boundary diffusion process of Nd-Fe-B magnets, J. Magn. Magn. Mater. 514 (2020) 167227.
[21] H. Nakamura, K. Hirota, T. Ohashi, T. Minowa, Coercivity distributions in Nd–Fe–B sintered magnets produced by the grain boundary diffusion process, J. Phys. D: Appl. Phys. 44 (6) (2011) 064003.
[22] Y. Wang, M. Zhu, Q. Sun, F. Xia, J. Zuo, Y. Wu, X. Song, Z. Li, High-quality TbF3 coating prepared by suspension plasma spraying technique for improving the grain boundary diffusion efficiency of sintered Nd-Fe-B magnets, Surf. Coat. Technol. 465 (2023) 129575.
[23] Y.J. Wong, H.W. Chang, Y.I. Lee, W.C. Chang, C.H. Chiu, C.C. Mo, Coercivity enhancement of thicker sintered NdFeB magnets by grain boundary diffusion with low-melting Tb75−xCexCu25 (x = 0–45) alloys, J. Magn. Magn. Mater. 515 (2020) 167287.
[24] M. Itakura, M. Namura, M. Nishida, H. Nakamura, Elemental distribution near the grain boundary in a Nd–Fe–B sintered magnet subjected to grain-boundary diffusion with Dy2O3, Mater. Trans. 61 (3) (2020) 438–443.
[25] T.H. Kim, T.T. Sasaki, T. Ohkubo, Y. Takada, A. Kato, Y. Kaneko, K. Hono, Microstructure and coercivity of grain boundary diffusion processed Dy-free and Dy-containing NdFeB sintered magnets, Acta Mater. 172 (2019) 139–149.
[26] T. Zhou, Y. Guo, G. Xie, S.U. Rehman, R. Liu, J. Liu, P. Qu, M. Li, Coercivity and thermal stability enhancement of NdFeB magnet by grain boundary diffusion Tb80Al20 alloys, Intermetallics 138 (2021) 107335.
[27] T. Zhou, P. Qu, W. Pan, R. Liu, M. Li, S.U. Rehman, Z. Zhong, G. Xie, Sintered NdFeB magnets with Tb - Dy double-layer core/shell structure were fabricated by double alloy method and grain boundary diffusion, J. Alloys Compd. 856 (2021) 158191.
[28] Y.J. Wong, W.C. Hsu, H.W. Chang, Y.I. Lee, W.C. Chang, C.H. Chiu, C.C. Mo, Comparison on the coercivity enhancement of the sintered NdFeB magnets by grain boundary diffusion with Tb70Cu30 powders prepared by different milling methods, AIP Adv. 11 (2) (2021) 025101.
[29] W. Mo, L. Zhang, Q. Liu, A. Shan, J. Wu, M. Komuro, Dependence of the crystal structure of the Nd-rich phase on oxygen content in an Nd–Fe–B sintered magnet, Scr. Mater. 59 (2) (2008) 179–182.
[30] T.-H. Kim, S.-R. Lee, S. Namkumg, T.-S. Jang, A study on the Nd-rich phase evolution in the Nd–Fe–B sintered magnet and its mechanism during post-sintering annealing, J. Alloys Compd. 537 (2012) 261–268.
[31] F. Xu, J. Wang, X. Dong, L. Zhang, J. Wu, Grain boundary microstructure in DyF3-diffusion processed Nd–Fe–B sintered magnets, J. Alloys Compd. 509 (30) (2011) 7909–7914.
[32] Y.J. Wong, H.W. Chang, Y.I. Lee, W.C. Chang, C.H. Chiu, C.C. Mo, Comparison on the coercivity enhancement of sintered NdFeB magnets by grain boundary diffusion with low-melting (Tb, R)75Cu25 alloys (R= None, Y, La, and Ce), AIP Adv. 9 (12) (2019) 125238.
[33] G. Ding, S. Liao, J. Di, B. Zheng, S. Guo, R. Chen, A. Yan, Microstructure of core-shell NdY-Fe-B sintered magnets with a high coercivity and excellent thermal stability, Acta Mater. 194 (2020) 547–557.
[34] Y.L. Huang, Q. Rao, Q. Feng, Z.J. Wu, Y.F. Yao, Y.H. Hou, W. Li, J.M. Luo, An insight into the improved microstructure and elevated comprehensive properties of sintered Nd-Fe-B magnets via the infiltration of DyCu alloy, J. Mater. Res. Technol. 20 (2022) 3094–3102.
[35] S. Kim, H.-S. Lee, W.H. Nam, D. Kim, W.H. Shin, J.W. Roh, W. Lee, Enhancement of thermal stability of Nd–Fe–B sintered magnets with tuned Tb-diffused microstructures via temperature control, J. Alloys Compd. 855 (2021) 157478.
[36] T.-H. Kim, S.-R. Lee, S.J. Yun, S.H. Lim, H.-J. Kim, M.-W. Lee, T.-S. Jang, Anisotropic diffusion mechanism in grain boundary diffusion processed Nd–Fe–B sintered magnet, Acta Mater. 112 (2016) 59–66.
[37] Y. Zhao, H. Feng, A. Li, W. Li, Diffusion temperature dependent microstructure and magnetic properties of TbHx grain boundary diffused Nd–Fe–B magnets, AIP Adv. 11 (2) (2021) 025208.
[38] M. Tang, X. Bao, K. Lu, L. Sun, X. Mu, J. Li, X. Gao, Microstructure modification and coercivity enhancement of Nd-Ce-Fe-B sintered magnets by grain boundary diffusing Nd-Dy-Al alloy, J. Magn. Magn. Mater. 442 (2017) 338–342.
[39] U.M.R. Seelam, T. Ohkubo, T. Abe, S. Hirosawa, K. Hono, Faceted shell structure in grain boundary diffusion-processed sintered Nd–Fe–B magnets, J. Alloys Compd. 617 (2014) 884–892.